Dipole glassy state evidence for $CuInP_2(Se_xS_{1-x})_6$ ferrielectric mixed crystals from Raman scattering and optical absorption data

Beley L.M., Mykajlo O.A., Stephanovych V.O., Studenjak I.P.,
Gurzan M.I. and Vysochanskii Yu.M.

Institute of Solid State Physics and Chemistry, Uzhgorod University,
46 Pidgirna St., 88000 Uzhgorod, Ukraine
e-mail: vysochanskii@univ.uzhgorod.ua

Received: 20.01.2007

Abstract

The temperature and concentration dependences of Raman scattering and optical absorption spectra for $CuInP_2(Se_xS_{1-x})_6$ crystals are investigated. Similarly to dynamic disordering of Cu^+ ions at the transition from ferrielectric into paraelectric phase for $CuInP_2S_6$ compound, static disordering of these ions in the mixed crystals in the dipole glassy state at low temperatures determines rise in the phonon damping and increase in the energetic width w of exponential optical absorption edge. The concentration and temperature dependences $w(T,x)$ clearly reveal "asymmetry" of the dipole ordering on T–x phase diagram: the dipole glassy state smoothly evolves into ferrielectric one, coexisting with the latter under decrease of selenium content till $x = 0$. The dipole glassy state sharply transforms into ferrielectric phase with growing selenium concentration, passing through the relaxor state in the region of $x \approx 0.7$–0.8.

Keywords: ferrielectrics, dipole glass, $CuInP_2S(Se)_6$, Raman scattering, optical absorption

PACS: 77.80.Bh, 78.40.Ha, 61.82.Fk, 78.40.Fy, 78.40.Pg

1. Introduction

Layered $CuInP_2S_6$ crystals are ferrielectrics with two cation sublattices associated with indium and copper. A complicated relaxational dynamics of copper ions accompanies the first-order phase transition (PT) of order-disorder type characterized with the symmetry change $C2/c \rightarrow Cc$. Spontaneous polarization at $T < T_c \approx 310$ K is normal to the layer planes. Polarity of the ferrielectric phase is determined by anti-collinear polarity of copper and indium sublattices, i.e. by "upward" temperature displacements (hoppings) of the copper atoms from the octahedral centres and "downward" displacements of the indium atoms [1].

The symmetry reduction $P\bar{3}1c \rightarrow P31c$ at $T < T_c = 225$ K has been observed in $CuInP_2Se_6$ crystals [2]. Similarly to $CuInP_2S_6$, the relaxational dynamics of copper ions is also observed in the selenide compound. An important feature of selenides is higher covalence degree of their bonds. These facts enable us to assume that the potential relief for the copper ions in $CuInP_2Se_6$ should be flatter than that for the sulfide analog, and this has been confirmed experimentally [2,3]. Evidently, for this reason the PT in the selenide compound is observed at lower temperature than for the sulfide compound.

The PTs in the compounds under consideration are triggered by cooperative freezing of intersite copper motions. This cooperative dipolar behaviour is supposed [4] to arise from the presence of off-centring displacement caused by electronic instability, in the form of a second-order Jahn-Teller (SOJT) effect related to d^{10} electronic configuration of the Cu^+ cations. The SOJT coupling, involving the localized d^{10} states that form the top of the valence band and the *s-p* states of the bottom of the conduction band, is predicted to yield such the instability.

In addition to the role of Cu^+ ions mentioned above, the highest valence bands for the layered $M_2P_2S_6$ compounds are also known [4,5] to be formed by (P-P)*p* bonding states and nonbonding S3*p* levels, while the lowest conduction bands are mostly constituted by anti-bonding (P-P)*p* and bonding and anti-bonding S*p* states. Therefore, the optical absorption edge in $CuInP_2S_6$ crystals can be formed by the electronic transitions between the (P-P)*p* bonding and anti-bonding states, too. Redistribution of the copper atoms over different positions in a multi-well potential results in essential nonequivalence of structural P_2S_6 groups, enabling both the S-P and P-P bond lengths and the S-P-S and S-P-P angles to be varied within a certain interval. This is confirmed by substantial increase in the damping of internal stretching of $(P_2S_6)^{4-}$ anion and valence vibration lines in the Raman spectra, observed with increasing temperature above the PT point to the paraelectric phase [6]. The hopping motion of the copper cation also gives rise to variations of the S-P and P-P bonds characteristics, leading to smearing of optical absorption edge, and so deviation from the spectral dependence typical for direct transitions, in the ferrielectric phase and appearance of exponential absorption tails in the paraelectric phase of $CuInP_2S_6$ [7]. Similar broadening of the Urbach optical absorption edge at the PT into paraelectric phase has also been observed for the $CuInP_2Se_6$ compound [8].

Different types of dipole ordering have been observed for the mixed $CuInP_2(Se_xS_{1-x})_6$ crystals [9,10]. So, a dipole glassy state appears in the middle of the concentration interval [11–13]. With increasing selenium content, the dipole glassy state transforms into ferrielectric phase, through a relaxor state. When the sulfur concentration grows, the dipole glassy state coexists with the ferrielectric phase.

The aim of this paper is to investigate structural disordering in the mixed $CuInP_2(Se_xS_{1-x})_6$ crystals related to appearance of the dipole glassy state, using the Raman scattering and the optical absorption techniques.

2. Phase diagram for the mixed $CuInP_2(Se_xS_{1-x})_6$ crystals

Hopping motion of the copper cations in the mixed crystals occurs in the local potential determined by different combinations of the nearest chalcogen atoms. Strong smearing of the PTs in $CuInP_2(Se_xS_{1-x})_6$ solid solutions could be explained just by this fact [10].

According to the dielectric spectroscopy data [12–14], the first-order PT in $CuInP_2S_6$ is strongly smeared when sulfur is substituted by selenium and the correlated “freezing” of relaxational hopping dynamics of the Cu^+ ions is destroyed. Then the dipole glassy state appears at cooling and takes place till the concentration $x = 0.6$. When the concentration varies in the region $x = 0.75–0.80$, the dipole glassy state in the mixed crystals transforms again into the ferrielectric phase and a clear enough PT is observed at $x > 0.8$ (see Fig. 1).

It is worth mentioning that the relaxor ferrielectric state obviously appears in the range of $0.75 < x < 0.80$ [14]. One can assume that micro(nano)-clusters of spontaneous polarization in this state rapidly grow with increasing selenium concentration.

Thus, three regions could be distinguished on the phase diagram of the solid solutions $CuInP_2(Se_xS_{1-x})_6$. In the region of $0 \le x \le 0.3$ the monoclinic structure exists [11]. Here partial substitution of sulfur by selenium modifies strongly the local potential for Cu^+ ions. As a result, the temperature T_c of the first-order paraelectric-to-ferrielectric PT is lowered rapidly. This PT is also strongly smeared: already at $x = 0.05$ it appears as a wide maximum on the temperature dependence of dielectric susceptibility [10]. Obviously, the regions of correlated “freezing” of the hopping dynamics of Cu^+ ions get substantially narrower with increasing selenium concentration and so the ferrielectric phase transforms into the dipole glassy state. Furthermore, the PT from the monoclinic structure *Cc* to the “more compact” trigonal *P*31*c* one promotes a development of nonequivalence of the local potentials for the copper ions.

A statistical distribution of S and Se atoms is realized in the considered solid solutions [15]. Acentric quasi-trigonal positions of the copper ions are located near the

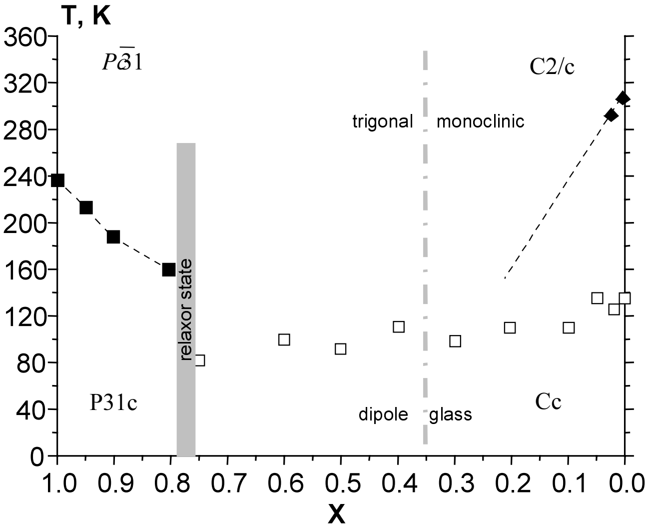

Fig. 1. Phase diagram of mixed $CuInP_2(Se_xS_{1-x})_6$ crystals [10,11]. Dark diamonds: the first-order PTs; dotted line: possible location of the smeared first-order PTs between the monoclinic phases; dark squares: PTs between the trigonal phases; dashed vertical line: morphotropic phase boundary between the monoclinic and trigonal phases; shaded field: the relaxor state; open squares: temperatures of relaxational “freezing” anomalies in the low-frequency (10^4 Hz) dielectric permittivity, which are related to the dipole glassy state.

layers of chalcogen atoms. These conditions apparently determine a wide-ranged distribution of local potential characteristics of the copper ions mentioned before.

The dipole glassy state in our solid solutions occupies a middle of the concentration range. Nonetheless, while the ferrielectric state continuously transforms to the dipole glassy one at a partial substitution of sulfur atoms by selenium ones, a further increase in the selenium content leads to the situation when the dipole glass again transforms, in a threshold way, to the ferrielectric phase, evidently through the relaxor state [14]. Such the concentration behaviour could be predetermined by smaller dimensions of sulfur atoms, if compare to the selenium ones. When the selenium is partially substituted by sulfur in $CuInP_2Se_6$, the latter atoms not so strongly change the local potential for the Cu^+ ions, but only till the threshold concentration region of $x = 0.75–0.80$.

3. Experiments and discussions

3.1. Raman scattering

The temperature dependence of the Raman scattering spectra for $CuInP_2(Se_xS_{1-x})_6$ mixed crystals have been studied the same way as earlier described for $CuInP_2S_6$ crystals [6]. The samples have been grown with a vapour transport method [6,10].

The spectral lines for the crystals under test (see Fig. 2) could be identified in the following manner [6]. The spectral lines placed higher than 150 cm^{-1} could be related to the internal vibrations of $(P_2S_6)^{4-}$ anions. The valence vibrations of the P-P bonds are placed near 378 cm^{-1}. The S–P–S deformation modes and the slope or tilt vibrations for PS_3 groups are located in the region of 150–300 cm^{-1}. Increase in the anion mass occurring at the substitution S → Se determines lowering frequency border between the internal and external vibrations down to 100 cm^{-1}. At the same time, the frequency of the valence vibrations of P-P bonds decreases to 220 cm^{-1} [15].

Partial substitution of sulfur by selenium in the solid solutions $CuInP_2(Se_xS_{1-x})_6$ gives also rise to additional spectral lines in the frequency region of internal valence

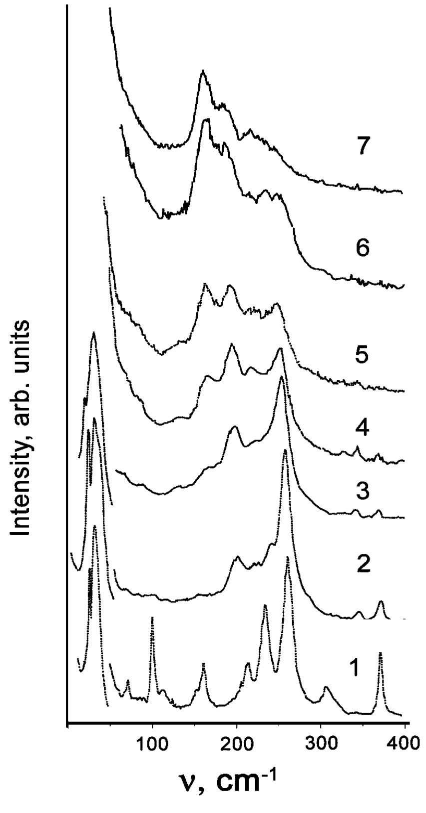

Fig. 2. Raman scattering spectra for the mixed $CuInP_2(Se_xS_{1-x})_6$ crystals at 295 K $x = 0 – 1, 0.1 – 2, 0.2 – 3, 0.3 – 4, 0.35 – 5, 0.4 – 6$ and $0.5 – 7$.

vibrations of $[P_2S(Se)_6]^{4-}$ anions, which appear due to changing effective mass of structural groups. For example, increasing selenium concentration x induces decrease in the intensity of spectral line localized near 378 cm^{-1}, whereas the intensity of the line close to 343 cm^{-1} then increases (see Fig. 3). Such a redistribution of spectral line intensities should be associated with the appearance of some anions, in which sulfur is partly substituted by selenium, e.g., $(P_2S_5Se)^{4-}$ anions.

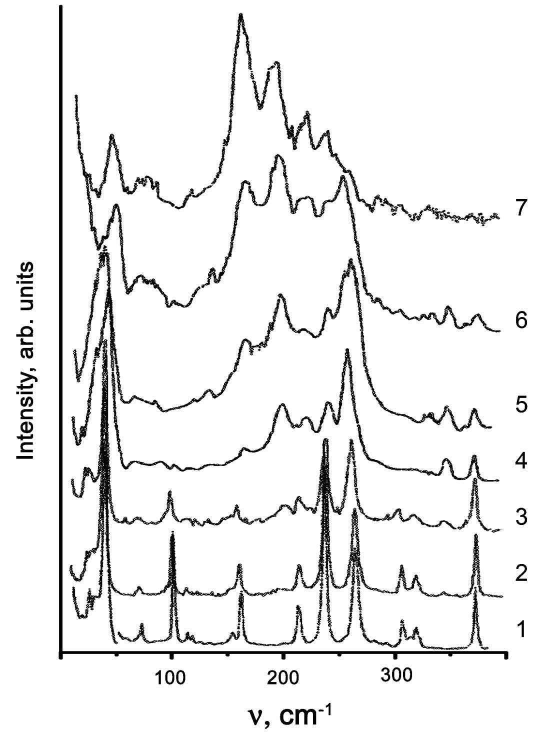

Fig. 3. Raman scattering spectra for the mixed $CuInP_2(Se_xS_{1-x})_6$ crystals at 115 K: $x = 0$ – 1, 0.02 – 2, 0.05 – 3, 0.2 – 4, 0.3 – 5, 0.35 – 6 and 0.5 – 7.

In general, the Raman spectroscopy data reveal that the chalcogen atoms in the solutions $CuInP_2(Se_xS_{1-x})_6$ are statistically distributed over the crystal lattice sites and so these solutions are of the replacement type [15].

At high concentrations of selenium the number of spectral lines in the Raman spectra of our solid solutions decreases. This evolution is caused by the change in the symmetry of structure from monoclinic (at $x < 0.2$) to trigonal (at $x > 0.4$) [11]. In the paraelectric phase of $CuInP_2S_6$ crystal (the symmetry $C2/c$) the $14A_g + 16B_g$ modes could be active in the Raman scattering [6]. For the trigonal paraelectric phase in $CuInP_2Se_6$ crystal described by the symmetry group $P\overline{3}1c$, the quantity of the Raman-active modes becomes substantially smaller. Here only the vibrations $4A_{1g} + 6A_{2g} + 10E_g$ could be observed. Hence, the number of fully symmetrical modes decreases from 14 to 4. Indeed, only four lines are observed in the Raman spectra of the mixed crystal characterized with $x = 0.5$ (Fig. 2).

Substantial increase in the Raman spectral line widths is seen for the mixed crystals $CuInP_2(Se_xS_{1-x})_6$ with increasing selenium content. For the middle of the concentration range and low temperatures, the damping of the spectral lines (see Fig. 3) is comparable with that observed for the paraelectric phase in $CuInP_2S_6$ crystal [6]. When comparing the Raman spectra at 295 and 115 K (Fig. 2 and 3), we may estimate a temperature dependence of the damping for the spectral lines of internal valence vibrations (nearby 370 cm^{-1}) and the deformation modes (nearby 260 cm^{-1}) typical for the crystals with different x values. It is seen that, even at low temperatures, the damping of the optical phonons becomes very high when the selenium concentration increases. For the concentrations of selenium as small as $x = 0.02$, the width of the spectral line decreases notably at cooling into ferrielectric phase (lower than 290 K – see Fig. 4), while for the case of $x = 0.15$ we observe a strong damping of phonons which does not decrease at cooling (Fig. 5). The damping of phonons peculiar for the crystal with $x = 0.2$ at low temperatures is similar to that observed in the paraelectric phase of $CuInP_2S_6$ crystal (see Fig. 6).

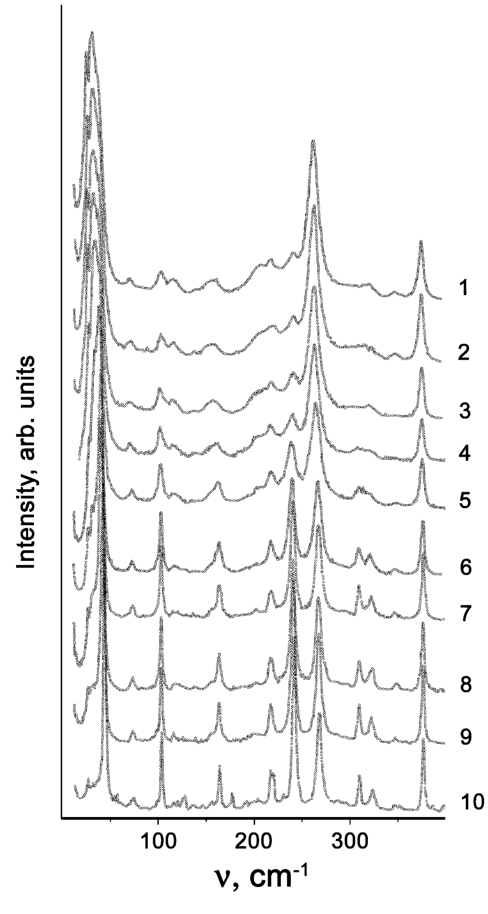

Fig. 4. Raman scattering spectra for the solid solution $CuInP_2(Se_xS_{1-x})_6$ ($x = 0.02$) at different temperatures: 1 – 310, 2 – 300, 3 – 295, 4 – 290, 5 – 280, 6 – 270, 7 – 150, 8 – 138, 9 – 115 and 10 – 81 K.

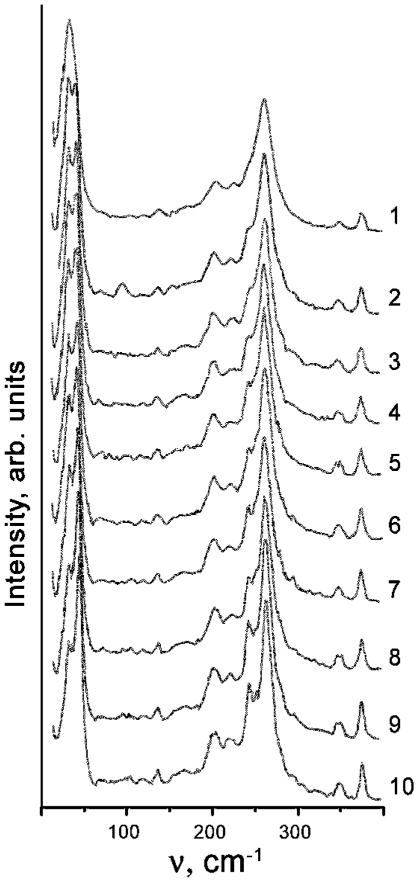

Fig. 5. Raman scattering spectra for the solid solution $CuInP_2(Se_xS_{1-x})_6$ ($x = 0.15$) at different temperatures: 1 – 293, 2 – 220, 3 – 210, 4 – 200, 5 – 195, 6 – 190, 7 – 185, 8 – 180, 9 – 150 and 10 – 138 K.

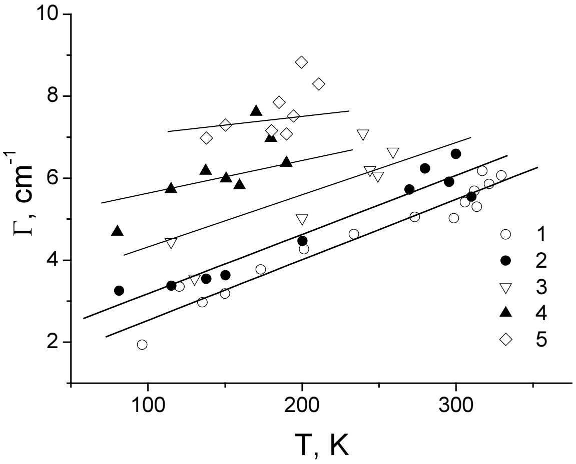

Fig. 6. Temperature dependences of damping parameters for the Raman spectral lines in $CuInP_2(Se_xS_{1-x})_6$ corresponding to the internal valence vibrations of $P_2S(Se)_6$ groups (the frequency is close to 378 cm^{-1}): $x = 0$ – 1, 0.02 – 2, 0.05 – 3, 0.15 – 4 and 0.20 – 5.

The behaviour of the Raman scattering spectra observed for the solid solutions $CuInP_2(Se_xS_{1-x})_6$ is certainly determined by a static disordering of the copper cations in the state of dipole glass occurring at the low temperatures. As mentioned earlier, the existence of the dipole glassy state has been confirmed by dielectric measurements [12–14]. This state produces a strong anharmonicity of the lattice dynamics, similarly to the case of dynamic disordering of copper cations in the paraelectric phase.

3.2. Optical absorption

The temperature dependences of optical absorption spectra for the mixed crystals $CuInP_2(Se_xS_{1-x})_6$ has been studied as described earlier for the $CuInP_2S_6$ and $CuInP_2Se_6$ compounds [7,8]. The absorption edge spectra obtained within the temperature region 77–325 K have exponential shape (see, e.g., the spectra in Fig. 7 derived for the crystals with $x = 0.2$). Their temperature dependence could be described with the empirical Urbach rule [16]:

$$\alpha(h\nu) = \alpha_o \cdot \exp\left[\frac{h\nu - E_0}{w}\right],$$

where $w = kT/\sigma$ denotes the energetic width of exponential absorption edge, the parameter σ is related to the constant of electron-phonon interaction, $h\nu$ is the photon energy and α_0, E_0 the coordinates of the intercept point for the Urbach absorption edges.

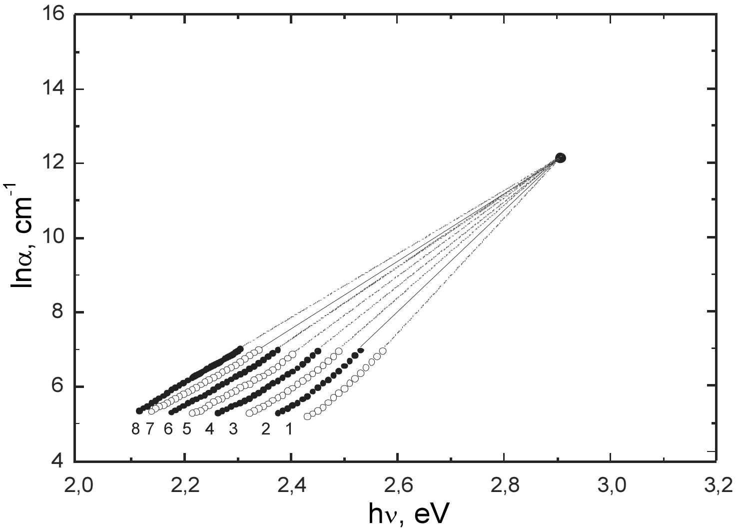

Fig. 7. Spectral dependences of the absorption coefficients α for $CuInP_2(Se_{0.20}S_{0.80})_6$ crystals at different temperatures: 1 – 77, 2 – 145, 3 – 183, 4 – 216, 5 – 245, 6 – 273, 7 – 299 and 8 – 325 K.

The temperature and concentration dependences of the Urbach absorption edge widths w for the mixed crystals with $x = 0.2$, 0.5 and 0.8 are shown in Fig. 8 and 9, respectively. The behaviour of $w(T,x)$ observed by us reflects a degree of disordering

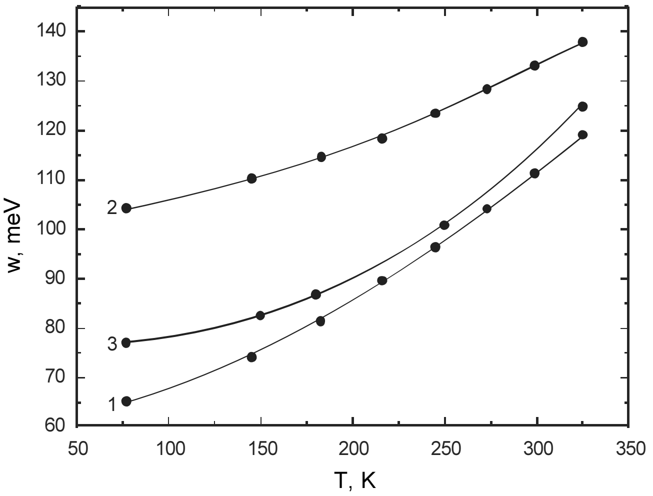

Fig. 8. Temperature dependences of the Urbach edge widths *w* for $CuInP_2(Se_{0.20}S_{0.80})_6$ (1), $CuInP_2(Se_{0.50}S_{0.50})_6$ (2) and $CuInP_2(Se_{0.80}S_{0.20})_6$ (3) crystals.

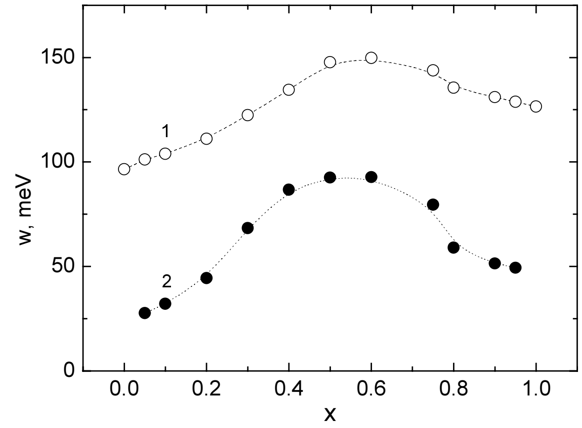

Fig. 9. Widths *w* of the Urbach edge at 325 K (1) and 77 K (2) as functions of the concentration *x* for the mixed $CuInP_2(Se_xS_{1-x})_6$ crystals.

occurred in the crystalline lattice. The smearing of the absorption edge is caused by intense temperature-dependent hopping of the copper ions between the potential wells, as well as their penetrating into the interlayer van der Waals space at high temperatures, which promotes the ionic conductivity [6]. The relaxational dynamics of Cu^+ cations involves essential anharmonicity of the internal vibrations of $(P_2S_6)^{4-}$ anions. By means of electron–phonon interaction, this modifies the bonding and anti-bonding (P-P)*p* states that participate in formation of the valence band top and the conduction band bottom. High values of the exponential absorption edge energy width *w* (more than 100 meV) are typical for glassy semiconductors. Perhaps, a certain “glassy behaviour” occurs in the paraelectric phase of $CuInP_2S_6$ and $CuInP_2Se_6$ crystals, resulting in a strong absorption edge broadening owing to the smeared tails of the density of electronic states in the gap [7,8].

Even a small fraction of atomic replacements S↔Se, on the sides of both $CuInP_2S_6$ and $CuInP_2Se_6$, induces compositional disordering of the crystal lattice and smearing of the optical absorption edge. The distribution of the electron density is then ‘drawn’ into the forbidden gap. The exponential absorption edge energy width w in the paraelectric phase has a maximum value at the middle of the concentration range. Really, the parameter w taken at 325 K increases from ≈ 105 meV at $x = 0$ to $\approx$ 150 meV at $x = 0.5$ and then decreases to $\approx$ 130 meV at $x = 1$ (see Fig. 9). The energetic width w at this temperature is high enough even for the pure compounds $CuInP_2S_6$ and $CuInP_2Se_6$. This is caused by hopping dynamics of Cu^+ in the multi-well potential, which should modify essentially the electron density distribution in the vicinity of chalcogen atoms and smear the energetic levels that form the top of the valence band and the bottom of the conductivity band. In frame of this model, one can understand that the smearing of the optical absorption edge (the parameter w) for $CuInP_2Se_6$ crystals is larger than for $CuInP_2S_6$ crystals, since the former have more dense trigonal structure and flatter potential relief for the Cu^+ ions.

The concentration dependence of w at low temperatures (see Fig. 9) reflects some features of the dipole ordering. The parameter w strongly decreases for the crystals of $CuInP_2S_6$ and $CuInP_2Se_6$ cooled down to 77 K (i.e., into the ferrielectric phase), which is related to “freezing” of the copper ions dynamics. When the sulfur atoms in the $CuInP_2S_6$ compound are partially substituted by the selenium ones, the parameter w increases more rapidly if compare with the same process at 325 K. It is important to mention that at $x = 0.5$ the energetic width w increases to 100 meV, i.e. almost to the w value characteristic for the pure $CuInP_2S_6$ at 325 K. This confirms the fact that the “freezing” of Cu^+ ions at 77 K is not correlated for the mixed crystals with $x = 0.5$ (i.e., for the dipole glassy state). Here the static disordering of the Cu^+ ions smears the optical absorption edge, similarly to the dynamical disordering of these ions occurring in the paraelectric phase. When the selenium concentration increases from $x = 0.75$ to 0.80, the parameter w decreases rapidly enough. This could be surely associated with the mentioned threshold transition from the dipole glassy state to the ferrielectric phase, through the intermediate relaxor state.

Conclusions

The dipole ordering in the solid solutions $CuInP_2(Se_xS_{1-x})_6$ becomes completely uncorrelated in the middle of the concentration range. The dipole glassy state exists for these x at low temperatures, which is characterized with statically disordered Cu^+ ions [12–14]. The Raman scattering and optical absorption spectra reveal that, similarly to the dynamic disordering of these ions in the paraelectric phase of $CuInP_2S_6$ compound, the static disordering of Cu^+ in the dipole glassy state gives rise to a pronounced phonon damping and increasing energetic width w of the exponential optical absorption edge. The concentration and temperature dependences of the parameter w clearly reveal “asymmetry” of the dipole ordering on the T–x phase diagram. The dipole glassy state evolves smoothly into the ferrielectric state, which coexists with the former at decreasing, down to $x = 0$, selenium content. When the selenium concentration increases, the dipole glassy state sharply transforms into the ferrielectric phase, through the intermediate relaxor state appearing in the region of $x \approx 0.7$–0.8.

References

1. Simon A, Ravez J, Maisonneuve V, Payen C and Cajipe V, 1994. Paraelectric-ferrielectric transition in the lamellar thiophosphate $CuInP_2S_6$. Chem. Matter. **6**: 1575–1582.
2. Bourdon X, Maisonneive V, Cajipe V, Payen C and Fischer J, 1999. Copper sublattice ordering in layered $CuMP_2Se_6$ (M = In, Cr). J. Alloys and Compounds. **283**: 122–127.
3. Maisonneuve V, Cajipe V, Simon A, Von Der Muhll and Ravez J, 1997. Ferrielectric ordering in lamellar $CuInP_2S_6$. Phys. Rev. B. **56**: 10860–10868.
4. Fagot-Revurat Y, Bourdon X, Bertran F, Cajipe V and Malterre D, 2003. Interplay between electronic and crystallographic instabilities in the low-dimensional ferroelectric $CuInP_2Se_6$ J. Phys.: Condens. Matter. **15**: 595–602.
5. Rushchanskii KZ, Vysochanskii YuM, Cajipe VB and Bourdon X, 2006. Influence of pressure on the structural, dynamical and electronic properties of the SnP_2S_6 layered crystal. Phys. Rev. B. **73**: 115115–115126.
6. Vysochanskii YuM, Stephanovich VA, Molnar AA, Cajipe VB and Bourdon X, 1998. Raman spectroscopy of the $CuInP_2S_6$ and SnP_2S_6 crystals lattice vibrations. Phys. Rev. B. **58**: 9119–9124.
7. Studenyak IP, Mitrovcij VV, Kovacs GySh, Gurzan MI, Mykajlo OA, Vysochanskii YuM and Cajipe VB, 2003. Disordering effect on optical absorption processes in $CuInP_2S_6$ ferroelectrics. Phys. Stat. Solidi (b) 263: 678–686.
8. Studenyak IP, Mykajlo OA, Stephanovich VO, Gurzan MI, Vysochanskii YuM and Cajipe VB, 2003. Phase transitions and optical absorption edge in layered ferrielectrics $CuInP_2Se_6$. Phys. Stat. Sol. (a) **198**: 487–494.
9. Vysochanskii YuM, Molnar AA, Gurzan MI, Cajipe VB and Bourdon X, 2000. Dielectric measurement study of lamellar $CuInP_2Se_6$: Successive transitions towards a ferroelectric state via an incommensurate phase. Solid State Commun. **115**: 13–17.
10. Vysochanskii YuM, Molnar AA, Gurzan MI and Cajipe VB, 2001. Phase transitions in $CuInP_2(Se_xS_{1-x})_6$ layered crystals. Ferroelectrics. **257**: 147–154.
11. Vysochanskii Yu, Beley L, Perechinskii S, Gurzan M, Molnar O, Mykajlo O, Tovt V and Stephanovich V, 2004. Phase transitions and disordering effects in $CuInP_2S(Se)_6$ layered ferrielectrics. Ferroelectrics. **298**: 361–366.
12. Maior MM, Vrabel VT, Pritz IP, Korda NF, Gurzan MI and Vysochanskii YuM, 2005. Dielectric properties of solid solutions $CuInP_2(Se_xS_{1-x})_6$. Fiz. Tverd. Tela. **47**: 1670–1675.
13. Banys J, Grigalaitis R, Macutkevic J, Brilingas A, Samulionis V, Grigas J and Vysochanskii Yu, 2005. Dipolar glass behaviour in mixed $CuInP_2(S_{0.7}Se_{0.3})_6$ crystals. Ferroelectrics. **318**: 163–168.

14. Vysochanskii YuM, Maior MM, Belej LM and Khoma MM, 2006. Phase transitions and relaxational dynamics in layered ferrielectrics $CuInP_2(Se_xS_{1-x})_6$. Abstract Book of 4th French and Ukrainian Meeting on Ferroelectricity. Amiens, 21–24 November, 2006.
15. Vysochanskii Yu, Yevych R, Beley L, Stephanovich V, Mytrovcij V, Mykajlo O, Molnar A and Gurzan M, 2003. Phonon spectra and phase transitions in $CuInP_2(Se_xS_{1-x})_6$ ferrielectrics. Ferroelectrics. **284**: 161–173.
16. Urbach F, 1953. The long-wavelength edge of photographic sensitivity and of the electronic absorption of solids**.** Phys. Rev. **92**: 1324.